ISSN 0031-918X, Physics of Metals and Metallography, 2023, Vol. 124, No. 2, pp. 109–117. © Pleiades Publishing, Ltd., 2023.
Russian Text © The Author(s), 2023, published in Fizika Metallov i Metallovedenie, 2023, Vol. 124, No. 2, pp. 117–125.

ELECTRICAL AND MAGNETIC PROPERTIES

Features of the Magnetic State of an Ordered Array of Ferromagnetic Ribbons

V. A. Orlov[a, b, *], R. Yu. Rudenko[a], A. V. Luk'yanenko[b], V. Yu. Yakovchuk[b], V. A. Komarov[b], V. S. Prokopenko[c], and I. N. Orlova[c]

[a] *Siberian Federal University, Krasnoyarsk, 660041 Russia*
[b] *Kirenskii Institute of Physics, Russian Academy of Sciences, Krasnoyarsk, 660036 Russia*
[c] *Astaf'ev Krasnoyrsk State Pedagogical University, Krasnoyarsk, 660049 Russia*
**e-mail: vaorlov@sfu-kras.ru*

Received September 21, 2022; revised November 20, 2022; accepted November 22, 2022

Abstract—The features of the magnetic state of an array of parallel oriented permalloy ribbons are discussed. The arrays are made by explosive lithography. The ribbons have a thickness of 180 nm, a width of 2.8 μm, and a length of about 4 mm. The distance between ribbons in different samples varies in the range from 300 nm to 4 μm. It is found that the ribbons in the regions far from the end faces are in a single-domain state with small-angle ripples, the magnetization distribution of which correlates with inhomogeneities of the ribbon side surfaces. Moreover, there is a distinct relationship in the spatial distribution of the ripples between adjacent ribbons with a relatively small distance between them. This makes it possible to evaluate the role of the magnetostatic coupling of magnetic subsystems of array elements and to estimate the characteristic value of the random stray field that pins the magnetization.

Keywords: magnetic domain wall, magnetic vortex, ferromagnetic ribbon
DOI: 10.1134/S0031918X22601780

INTRODUCTION

Low-dimensional objects like ferromagnetic micro- and nanoribbons are considered promising components of information storage devices and other new generation spintronics devices [1–4]. Interest in ribbons is attributable to several factors. In particular, it opens the possibility of multiplying the recording density with simultaneous miniaturization of devices. The solution of this dual problem makes it necessary to investigate the magnetic properties of not only individual nanoobjects, but also their arrays [5–9]. This inevitably leads to the need to study the influence of the interaction of magnetic subsystems of nanoobjects on the properties of arrays. This is especially important for high-performance devices and/or spintronics devices based on fast magnetization reversal processes [10–13].

In particular, bit carriers in new generation information storage devices are topological magnetization inhomogeneities in magnetic ribbons/wires, such as magnetic vortices/skyrmions and domain walls of various types [14–20]. It is important to develop a reliable method for controlling the magnetic state of such objects. As a rule, the procedure for writing and reading information is associated with controlled sliding of topological inhomogeneities, which is provoked by the presence of electromagnetic fields, spin-polarized currents, and other factors. The mobility of bit carriers is affected by structural defects, field inhomogeneities, etc. In particular, the static magnetic state and magnetization reversal processes are substantially affected by stray field inhomogeneities, the existence of which is responsible for surface defects (roughness) of nanowires/nanoribbons [21–25]. Moreover, the main interaction mechanism of magnetic subsystems of elements in arrays can be magnetostatic coupling through stray fields.

In this work, ordered arrays of ferromagnetic ribbons with different element repetition periods were experimentally studied.

EXPERIMENTAL

The explosive lithography method was used to obtain arrays of ribbons with parallel orientations. A layer of an AZ Nlof 2035 negative photoresist was deposited on a prepared silicon substrate. This photoresist was chosen because of its high thermal stability (up to 250°C) and high chemical resistance. The creation of a uniform film with a certain thickness is a stage in the formation of the resist mask. Centrifugation was used to perform this operation, which makes

it possible to obtain uniform films (deviations from the average thickness along the surface are not more than ±10%). The substrate is fixed in a centrifuge with a vacuum suction cup and spun at a speed of 3000 rpm after applying a few drops of resist on it. The planarizing effect of centrifugal forces leads to the formation of supersmooth films with a thickness uniformity of about 1%, which cannot be achieved in any other way. After this, the films were exposed to light through a preliminarily prepared photomask. At the exposure stage, a DRSh-350 mercury lamp characterized by high radiation intensity and high parallelism and uniformity of the light beam was used as a source of actinic electromagnetic radiation. Next, the sample was washed in a developing solution that removed the photoresist with an unchanged structure. After this, a film of the 80NKhS alloy was deposited on a substrate covered with a photoresist by the thermal evaporation method in a high vacuum. After depositing the coating, the sample is immersed in an organic solvent, which dissolves the photoresist and removes it from the semiconductor surface. At the same time, unnecessary layers of deposited metal are removed along with the photoresist.

In this fashion, arrays of ribbons with a size of the order of 4×4 mm^2 were obtained. The thickness of the ribbons was $b = 180$ nm. The distance between ribbons in different arrays varied in the range from 4 to 0.3 μm. Figure 1 shows the morphological textures of the samples according to scanning probe force microscopy. Figure 2 shows an example of the morphology of the ribbons at their ends. These regions have features in the shape of a fork.

The state of magnetization was studied by magnetic force microscopy (MFM) on a Veeco MultiMode NanoScope IIIa SPM System microscope using a double-scan technique in the mode of frequency recording as an MFM contrast. The details of the magnetic state of the array are discussed in the next section.

RESULTS AND DISCUSSION

As found from the analysis of magnetic force microscopy data, the ribbons are practically in a single domain state (magnetization orientation along the long axis predominates) with the flux closing at the ends of the ribbons by combined domain walls containing magnetic vortices (see Fig. 3).

The vortex and quasi-vortex distribution of magnetization at the edges of the ribbons is facilitated by a dendritic shape with semicircle elements. In [27–29], diagrams that determine the ratios of the linear sizes of nanosized magnets were obtained theoretically and by computer simulation, in which various types of magnetic states are considered (magnetic vortex, magnetization in the plane, magnetization perpendicular to the plane, etc.). According to the data from [27–29], the ratio of the thickness b to the characteristic curvature radius R at the ribbon boundary (in our case, $b/R \approx 0.3$) corresponds to the state of a magnetic vortex or a vortex domain wall. This is actually confirmed by microscopy data.

We assume that the vortex objects, which are formed at the ends of the ribbons and separate the domains, begin to move by shifting along the long axis of the ribbons when the field is turned on. At the same time, the vortex walls move in a random potential of stray fields created by surface irregularities. This is a dominant mechanism of the process of magnetization reversal of ribbons [30].

At a distance from the end faces, a magnetization ripple is observed, which practically repeats the roughness of the side surfaces of the ribbons (see Fig. 4). Therefore, we attribute the existence of this ripple to the inhomogeneities of the side surfaces of the ribbons, in which stray fields arise. This is true for the samples shown in Figs. 1a and 1b, in which the distance between the ribbons is relatively large, so the role of the interaction of magnetic subsystems of different ribbons is insignificant.

An analysis of the contrast showed that the angular spread of the magnetization direction at a distance from the end faces does not exceed ±20°. This estimate was obtained from the analysis of the MFM image by drawing a cross section along the axis of the ribbon (cross section analysis). Figure 5 shows an example of the cross section analysis for the sample shown in Fig. 1b, on the basis of which the relationship between the magnetization misorientation angle and the frequency was determined. Between the regions with the maximum frequency difference in the cross section, which equals $\Delta\nu = 1.2$ Hz, a maximum angle between the magnetization vectors is also observed. Upon rotating the magnetic moment by approximately 90°, the frequency difference is $\Delta\nu = 2.5$ Hz. This relationship between the angle and the frequency was established by analyzing the MFM image at the edge of the same ribbon (see Fig. 6), for which the angular distribution of magnetization is known, for example, in a magnetic vortex near the end face.

It is important that the distributions of magnetization ripples in different ribbons of the arrays with closely spaced ribbons (Figs. 1c and 1d) noticeably correlate (see Fig. 7), which allows us to conclude that there is a significant magnetostatic coupling mechanism between magnetic subsystems through stray fields on the inhomogeneities of the side surfaces. This makes it possible to estimate the average constant of effective random anisotropy, which plays the role of a pinning factor associated with surface defects.

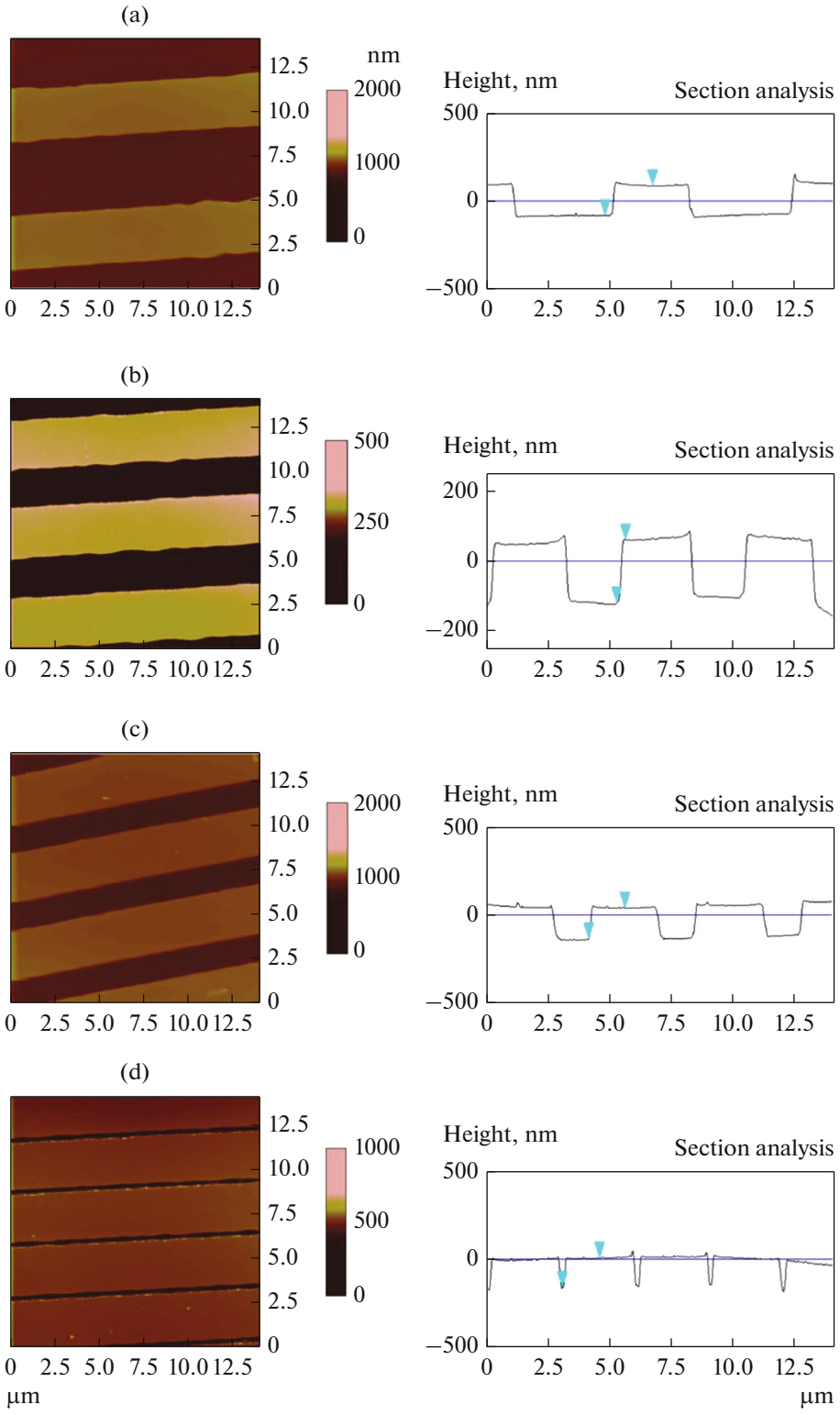

Fig. 1. The morphology of ordered arrays of ribbons. The images are taken from the regions far from the ends of the ribbons with a width of 2.8 μm; the distances between the ribbons are about (a) ≈4, (b) ≈2, (c) ≈1.5, and (d) ≈0.3 μm.

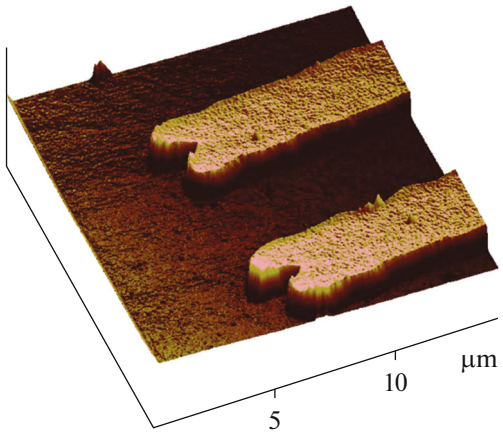

Fig. 2. The morphology of the ribbons at the end faces.

In [31], a theoretical method was proposed for estimating the stray fields created by the surface roughness of a ferromagnet. This method was developed in [32, 33] with respect to models with randomly distributed irregularities. According to [31–33], the field created by irregularities can be estimated using the following expression:

$$H = M_S \frac{\pi^2}{\sqrt{2}} \frac{h^2}{\lambda L} \exp\left(-\frac{2\pi d\sqrt{2}}{\lambda}\right). \quad (1)$$

Here, M_S is the saturation magnetization; h and λ are the average depth of irregularities and the average period of their repetition, respectively; L is the width of the magnet (the width of the ribbons); and d is the width of the nonmagnetic gap (the distance between the ribbons).

The random anisotropy constant K_{ef} associated with the existence of stray fields can be estimated from the following simple reasoning. If there is a noticeable connection between the magnetization ripples of adjacent ribbons (as in Fig. 5), then the stray field in which the selected ribbon is located begins to win the competition with the pinning field of the effective anisotropy created by the roughness (these fields are comparable). Hence, the K_{ef} constant can be expressed as follows:

$$K_{ef} = H_M M_S. \quad (2)$$

Here, H_M is the stray field created by all array elements due to the long-range nature of the magnetostatic interaction. Assuming that all ribbons are magnetized in the same direction, H_M can be estimated by summing field (1) over the array:

$$H_M \approx 2M_S \frac{\pi^2}{\sqrt{2}} \frac{h^2}{\lambda L} \sum_{n=1}^{\infty} \exp\left(-\frac{2\pi d\sqrt{2}}{\lambda}\right) = M_S \sqrt{2} \frac{\pi^2 h^2}{\lambda L} \left(\exp\left(\frac{2\pi d\sqrt{2}}{\lambda}\right) - 1\right)^{-1}. \quad (3)$$

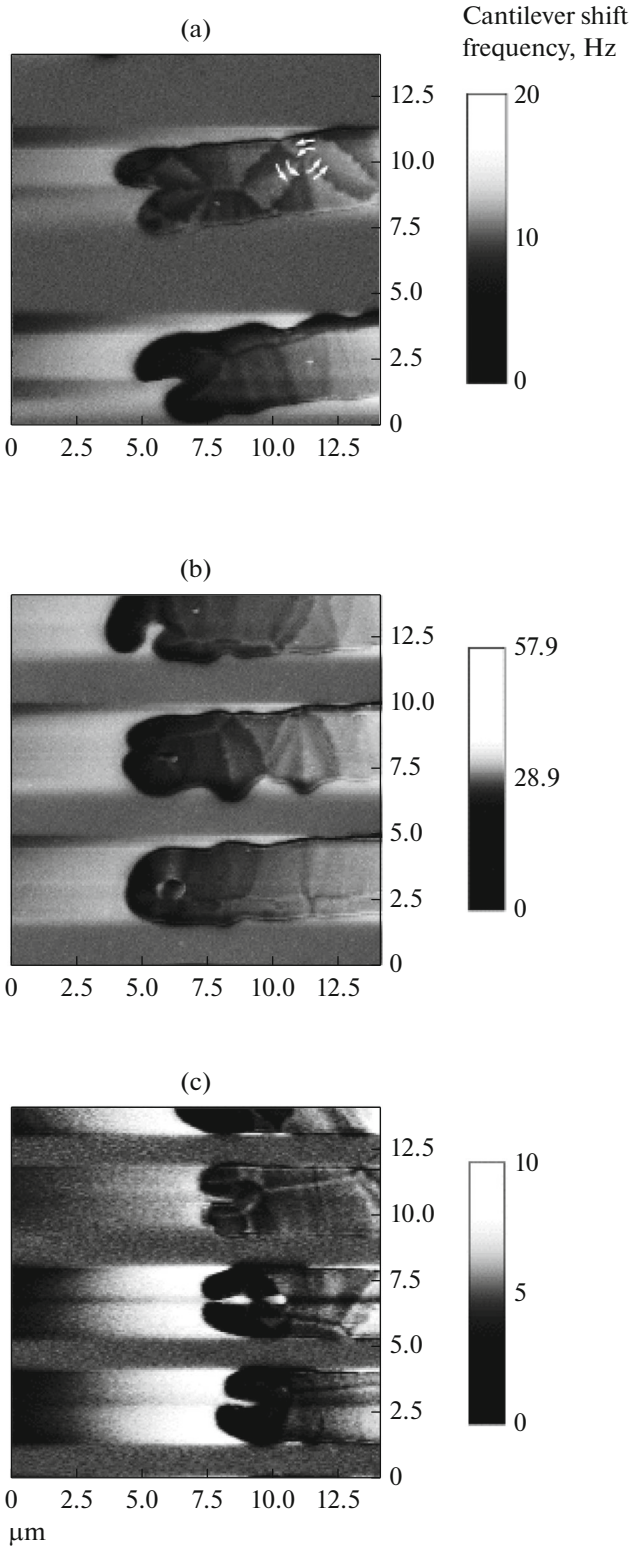

Fig. 3. The magnetic force contrast near the ribbon ends for the arrays shown in Figs. 1a–1c. The light arrows in Fig. 1a show the approximate orientation of the magnetization near the vortex formations.

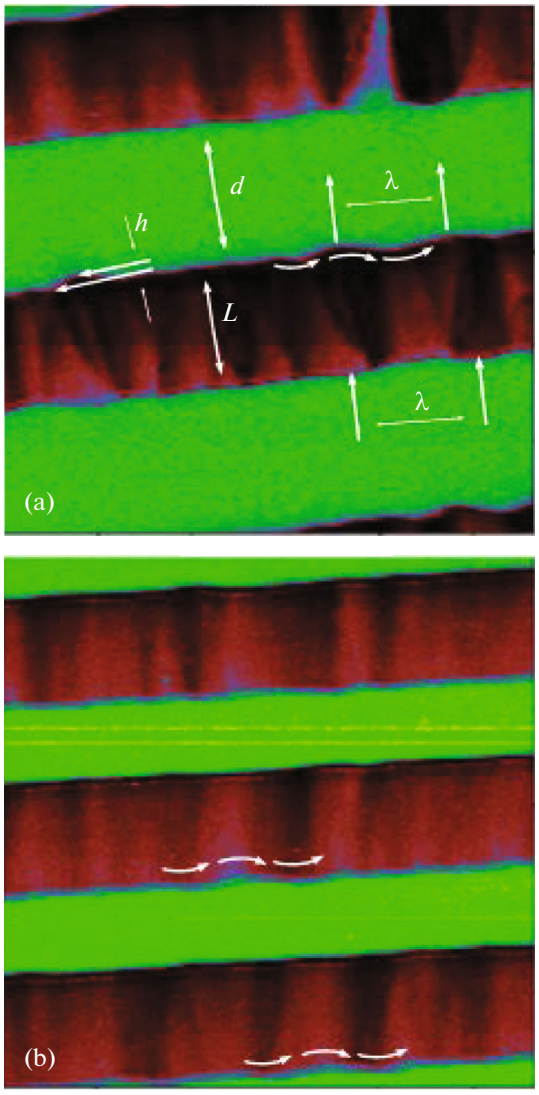

Fig. 4. The magnetic force contrast in the regions far from the ends of the ribbons for the arrays shown in Figs. 1a and 1b. The light arrows near the side surfaces show the approximate orientation of the magnetization.

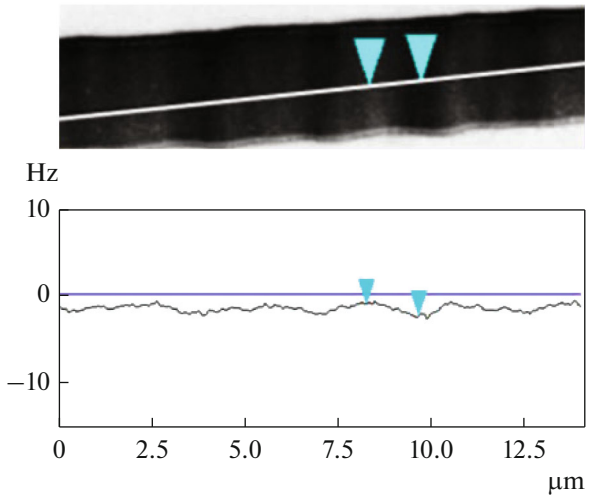

Fig. 5. An example of the result of a cross section analysis along the long axis of the ribbon in the region far from the end faces.

Noticeable weakening of the correlation between the magnetization ripples of the ribbons is observed for the sample shown in Fig. 5c. In the sample shown in Fig. 4b, this relationship is practically absent. Therefore, we can state that the distance d of interest to us in formula (3) approximately corresponds to the distance between the ribbons in the array shown in Fig. 1c ($d \approx 1.5$ μm). The characteristic value of roughness depths h is approximately 0.2 μm (see the upper part of Fig. 4), and the repetition period is $\lambda \approx 4$ μm (see Fig. 4). Taking into account these data from expressions (2) and (3), the constant is

$$K_{ef} \approx 0.026 M_S^2. \quad (4)$$

Within magnetic measurements, hysteresis loops were obtained by the Kerr method. The results are shown in Fig. 8. The linear size of the region covered by the measurement was about 3 μm. A laser with a round shape of the spot was used as a light source. The measurements were conducted in different regions of each of the samples. No differences were found in the hysteresis loops belonging to the same array, but recorded in different regions.

In the curves shown in Figs. 8b and 8c, constrictions, i.e., sections of the loop with a noticeable decrease in the coercive force relative to that for the loops of continuous films, are especially pronounced. Constricted graphs look like the loop is somewhat compressed along the field strength axis. This allows one to consider that the magnetization reversal similar to that in a system with two (or more) components occurs. In fact, no more than two or three ribbons partially fall into the region being measured by the Kerr method. Moreover, the distance between the ribbons in the arrays shown in Figs. 8b and 8c is not so large as to consider them noninteracting ribbons, but not so small that this interaction provides synchronous magnetization reversal similar to that observed in a continuous film. Features in the shape of constrictions barely appear in the curves shown in Figs. 8a and 8d. In fact, in the case of the array shown in Fig. 8a, only one ribbon falls into the measurement region (behaves like a continuous film), and in the case of the array shown in Fig. 8d, the magnetostatic coupling is so strong that the magnetization reversal occurs almost simultaneously (similar to a solid magnet). Relatively small values of the coercive force indirectly indicate that the process of nucleation and motion of vortex domain walls near the ends of the ribbons occurs in small fields compared, for example, to wires, in which the magnetization reversal process is provided by the sliding of traditional domain walls [34]. The main mechanism of

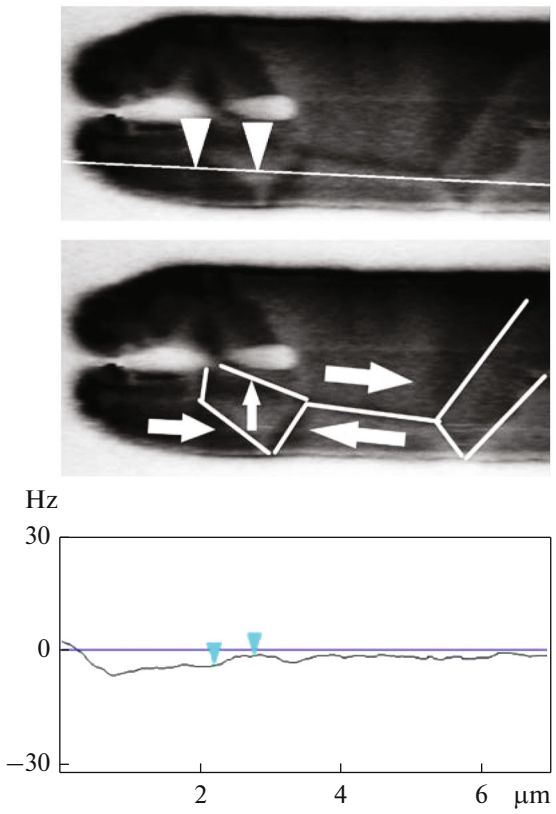

Fig. 6. An example of the result of a cross section analysis along the long axis of the ribbon near the end face.

magnetization reversal in the direction perpendicular to the ribbon axis (a lower row of plots in Fig. 8) is associated with the process of magnetization rotation. However, there are also features (constrictions) that we associate with the disappearance of the vortex structure with an increase in the field and upon approaching the saturation magnetization.

CONCLUSIONS

In summary, the magnetic force microscopy study of ordered two-dimensional arrays of ferromagnetic ribbons has shown that the equilibrium state is a practically homogeneous state of magnetization oriented along the long axis of the ribbons with superimposed small-angle ripples. The ripple period is determined by the period of inhomogeneities of the side surfaces of the ribbons. This statement is violated in arrays with a relatively small distance between the ribbons, where synchronization of the magnetization ripples of different ribbons is observed, regardless of the surface roughness positions. We associate the phenomenon of synchronization with the presence of stray fields induced by surface defects.

Structural inhomogeneities of the ribbons actually create a random potential in which domain walls move when the ribbons are remagnetized. Comparison of

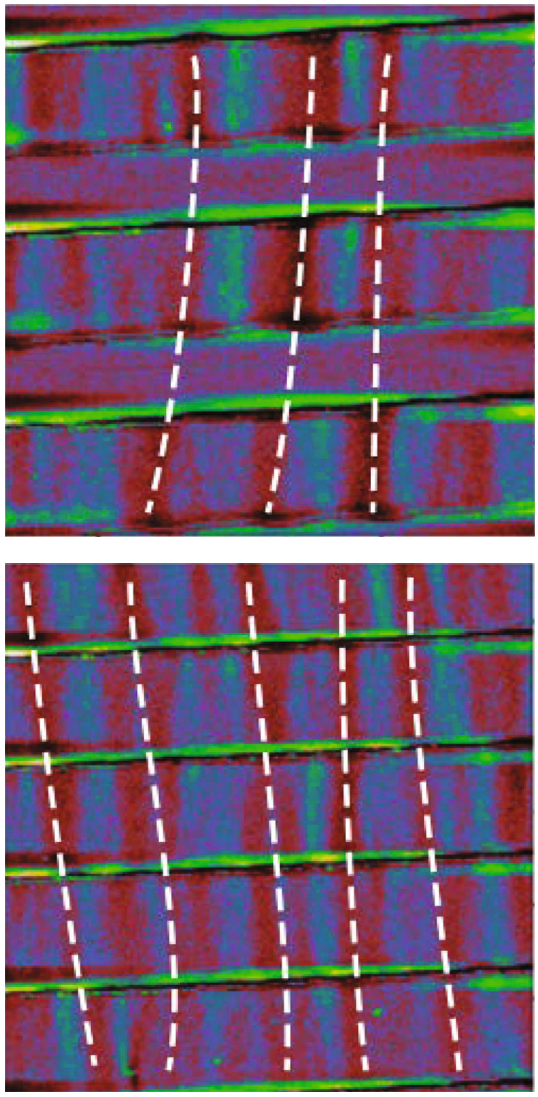

Fig. 7. The magnetic force contrast far from the ends of the ribbons for the arrays shown in Figs. 1c (upper image) and 1d (lower image). The light dash-and-dot lines show the synchronized sections of the magnetization ripples belonging to different ribbons.

the magnetic state of the samples with different distances between the components has made it possible to estimate the characteristic value of the random pinning field or the average constant of the random anisotropy induced by surface inhomogeneities.

It should be noted that the magnetic force microscopy images indicate the presence of vortex formations at the ends of the ribbons, which corresponds to the theoretical predictions for samples with the investigated geometric dimensions. We assume that the combined domain walls (a mixture of Néel turns and magnetic vortices) that appear at the ends of the ribbons begin to move and slide in a random potential created by stray fields in a way similar to the motion of

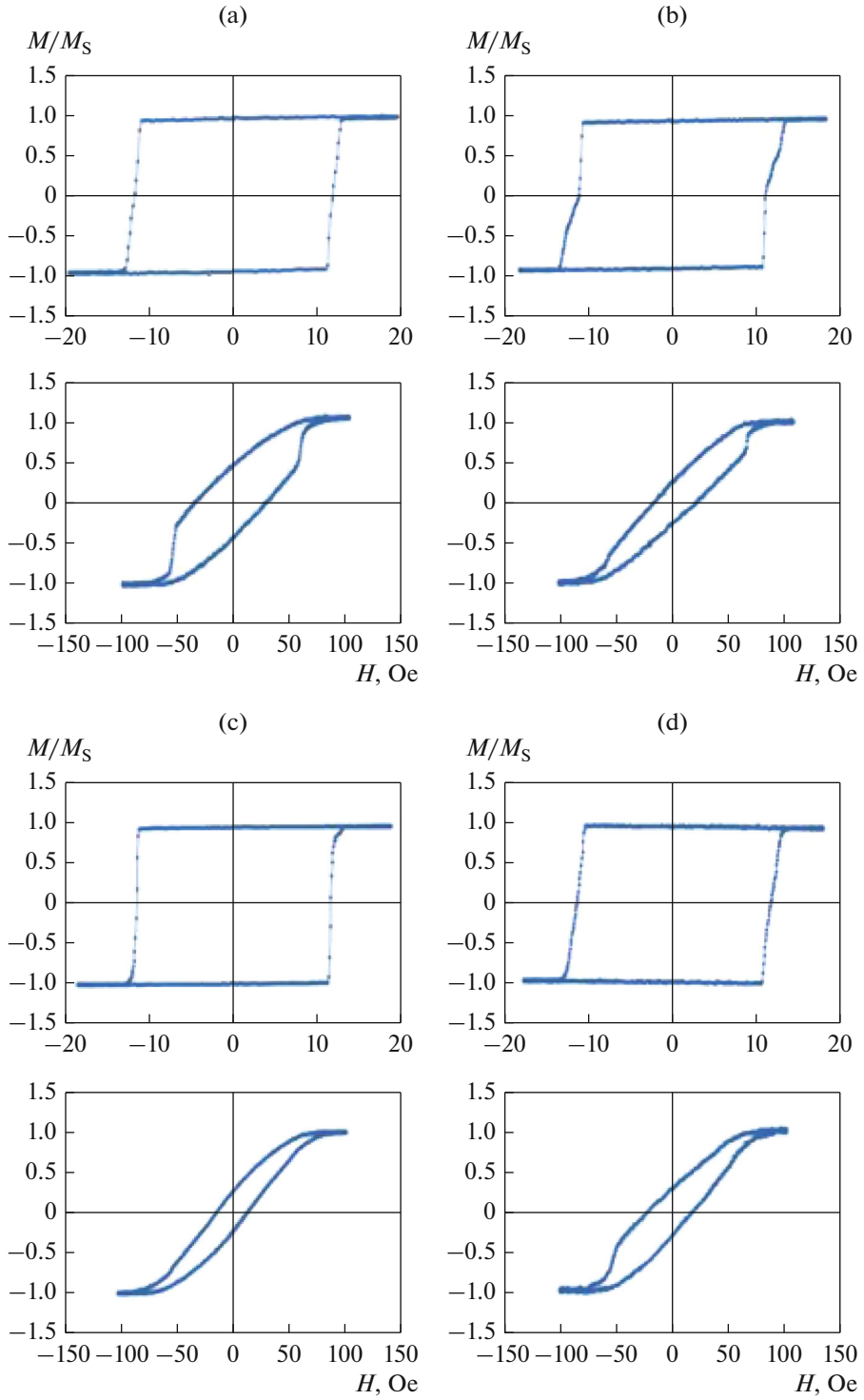

Fig. 8. Curves of the magnetization reversal of arrays. The left column of diagrams corresponds to the magnetization reversal along the long axis of the ribbons, and the right column corresponds to the magnetization reversal at a right angle to the axis of the ribbons in the plane of the arrays.

vortex walls in a random anisotropy field in the process of magnetization reversal [35].

Thus, it is reasonable to assume that the effects associated with the interaction between array elements have a substantial effect on the magnetic states. These effects should be taken into account when designing data storage devices, especially those based on arrays of densely packed elements.

FUNDING

In the part of sample preparations, this study was supported by the Russian Foundation for Basic Research within research project no. 20-02-00696. The magnetic measurements and theoretical calculations were performed within the framework of State assignment from the Ministry of Science and Higher Education of the Russian Federation (topic no. FSRZ-2020-0011).

CONFLICT OF INTEREST

The authors declare that they have no conflicts of interest.

REFERENCES

1. D. A. Allwood, G. Xiong, C. C. Faulkner, D. Atkinson, D. Petit, and R. P. Cowburn, "Magnetic domain-wall logic," Science **309**, 1688–1692 (2005). https://doi.org/10.1126/science.1108813
2. M. Hayashi, L. Thomas, R. Moriya, C. Rettner, and S. S. P. Parkin, "Current-controlled magnetic domain-wall nanowire shift register," Science **320**, 209–211 (2008). https://doi.org/10.1126/science.1154587
3. S. S. P. Parkin, M. Hayashi, and L. Thomas, "Magnetic domain-wall racetrack memory," Science **320**, 190–194 (2008). https://doi.org/10.1126/science.1145799
4. B. W. Walker, C. Cui, F. Garcia-Sanchez, J. A. C. Incorvia, X. Hu, J. S. Friedman, "Skyrmion logic clocked via voltage controlled magnetic anisotropy," Appl. Phys. Lett. **118**, 192404 (2021). https://doi.org/10.1063/5.0049024
5. J. -F. Song, J. P. Bird, and Y. Ochiai, "A nanowire magnetic memory cell based on a periodic magnetic superlattice," J. Phys.: Condens. Matter **17**, 5263–5268 (2005). https://doi.org/10.1088/0953-8984/17/34/011
6. A. G. Kozlov, M. E. Stebliy, A. V. Ognev, A. S. Samardak, A. V. Davydenko, and L. A. Chebotkevich, "Effective magnetic anisotropy manipulation by oblique deposition in magnetostatically coupled Co nanostrip arrays," J. Magn. Magn. Mater. **422**, 452–457 (2017). https://doi.org/10.1016/j.jmmm.2016.07.002
7. A. G. Kozlov, M. E. Stebliy, A. V. Ognev, A. S. Samardak, and L. A. Chebotkevich, "Micromagnetic structure of Co stripe arrays with tuned anisotropy," IEEE Trans. Magn. **51**, 2301604 (2015). https://doi.org/10.1109/TMAG.2015.2444594
8. I. Purnama, M. Chandra Sekhar, S. Goolaup, and W. S. Lew, "Current-induced coupled domain wall motions in a two-nanowire system," Appl. Phys. Lett. **99**, 152501 (2011). https://doi.org/10.1063/1.3650706
9. O. Iglesias-Freire, M. Jaafar, L. Pérez, O. de Abril, M. Vázquez, and A. Asenjo, "Domain configuration and magnetization switching in arrays of permalloy nanostripes," J. Magn. Magn. Mater. **355**, 152–157 (2014). https://doi.org/10.1016/j.jmmm.2013.12.012
10. S. Krishnia, I. Purnama, and W. S. Lew, "Remote Walker breakdown and coupling breaking in parallel nanowire systems," Appl. Phys. Lett. **105**, 042404 (2014). https://doi.org/10.1063/1.4891502
11. L. O'Brien, E. R. Lewis, A. Fernandez-Pacheco, D. Petit, R. P. Cowburn, J. Sampaio, and D. E. Read, "Dynamic oscillations of coupled domain walls," Phys. Rev. Lett. **108**, 187202 (2012). https://doi.org/10.1103/PhysRevLett.108.187202
12. Y. Su, J. Sun, J. Hu, and H. Lei, "Current-driven spring-like oscillatory motion of coupled vortex walls in a two-nanostripe system," Europhys. Lett. **103**, 67004 (2013). https://doi.org/10.1209/0295-5075/103/67004
13. A. T. Galkiewicz, L. O'Brien, P. S. Keatley, R. P. Cowburn, and P. A. Crowell, "Resonance in magnetostatically coupled transverse domain walls," Phys. Rev. B **90**, 024420 (2014). https://doi.org/10.1103/PhysRevB.90.024420
14. H. Youk, G.-W. Chern, K. Merit, B. Oppenheimer, O. Tchernyshyov, "Composite domain walls in flat nanomagnets: The magnetostatic limit," J. Appl. Phys. **99**, 101 (2006). https://doi.org/10.1063/1.2167049
15. N. Rougemaille, O. Fruchart, S. Pizzini, J. Vogel, and J. C. Toussaint, "Phase diagram of magnetic domain walls in spin valve nano-stripes," Appl. Phys. Lett. **100**, 172404 (2012). https://doi.org/10.1063/1.4704665
16. A. Thiaville and Yo. Nakatani, "Domain-wall dynamics in nanowires and nanostrips," in *Spin Dynamics in Confined Magnetic Structures III*, Ed. by B. Hillebrands and A. Thiaville, Topics in Applied Physics, Vol. 101 (Springer, Berlin, 2006), pp. 161–205. https://doi.org/10.1007/10938171_5
17. S. Jamet, N. Rougemaille, J. C. Toussaint, and O. Fruchart, "Head-to-head domain walls in one-dimensional nanostructures: An extended phase diagram ranging from strips to cylindrical wires, in *Magnetic Nano- and Microwires: Design, Synthesis, Properties and Applications*, Ed. by M. Vázquez, Woodhead Publishing Series in Electronic and Optical Materials (Woodhead Publishing, 2015), pp. 783–811. https://doi.org/10.1016/B978-0-08-100164-6.00025-4
18. A. Janutka, "Complexes of domain walls in ferromagnetic stripes," Acta Phys. Pol. A **124**, 641–648 (2013). https://doi.org/10.12693/APhysPolA.124.641
19. V. A. Orlov, A. A. Ivanov, and I. N. Orlova, "On the effect of magnetostatic interaction on the collective motion of vortex domain walls in a pair of nanostripes," Phys. Status Solidi B **256**, 1900113 (2019). https://doi.org/10.1002/pssb.201900113
20. V. D. Nguyen, O. Fruchart, S. Pizzini, J. Vogel, J.-C. Toussaint, N. Rougemaille, "Third type of domain wall in soft magnetic nanostrips," Sci. Rep. **5**, 12417 (2015). https://doi.org/10.1038/srep12417
21. A. A. Ivanov and V. A. Orlov, "A comparative analysis of the mechanisms of pinning of a domain wall in a nanowire," Phys. Solid State **53**, 2441–2449 (2011). https://doi.org/10.1134/S1063783411120079

22. L. K. Bogart, D. Atkinson, K. O'Shea, D. McGrouther, and S. McVitie, "Dependence of domain wall pinning potential landscapes on domain wall chirality and pinning site geometry in planar nanowires," Phys. Rev. B **79**, 054414 (2009). https://doi.org/10.1103/PhysRevB.79.054414

23. J. Brandão, L. K. Novak, H. Lozano, P. R. Soledade, A. Mello, F. Garcia, and L. C. Sampaio, "Control of the magnetic vortex chirality in permalloy nanowires with asymmetric notches," J. Appl. Phys. **116**, 193902 (2014). https://doi.org/10.1063/1.4902008

24. D. M. Burn, E. Arac, and D. Atkinson, "Magnetization switching and domain-wall propagation behavior in edge-modulated ferromagnetic nanowire structures," Phys. Rev. B **88**, 104422 (2013). https://doi.org/10.1103/PhysRevB.88.104422

25. K.-J. Kim, G.-H. Gim, J.-C. Lee, S.-M. Ahn, K.-S. Lee, Y. J. Cho, C.-W. Lee, S. Seo, K.-H. Shin, and S.-B. Choe, "Depinning field at notches of ferromagnetic nanowires with perpendicular magnetic anisotropy," IEEE Trans. Magn. **45**, 4056–4058 (2009). https://doi.org/10.1109/TMAG.2009.2024893

26. E. V. Vidal, Y. P. Ivanov, H. Mohammed, and J. Kosel, "A detailed study of magnetization reversal in individual Ni nanowires," Appl. Phys. Lett. **106**, 032403 (2015). https://doi.org/10.1063/1.4906108

27. K. Yu. Guslienko and V. Novosad, "Vortex state stability in soft magnetic cylindrical nanodots," J. Appl. Phys. **96**, 4451 (2004). https://doi.org/10.1063/1.1793327

28. W. Scholz, K. Yu. Guslienko, V. Novosad, D. Suess, T. Schrefl, R. W. Chantrell, and J. Fidler, "Transition from single-domain to vortex state in soft magnetic cylindrical nanodots," J. Magn. Magn. Mater. **266**, 155–163 (2003). https://doi.org/10.1016/S0304-8853(03)00466-9

29. N. Rougemaille, O. Fruchart, S. Pizzini, J. Vogel, J.-C. Toussaint, "Phase diagram of magnetic domain walls in spin valve nano-stripes," App. Phys. Lett. **100**, 172404 (2012). https://doi.org/10.1063/1.4704665

30. A. A. Ivanov and V. A. Orlov, "Scenarios of magnetization reversal of thin nanowires," Phys. Solid State **57**, 2204–2212 (2015). https://doi.org/10.1134/S1063783415110141

31. L. Néel, "Sur un nouveau mode de couplage entre les aimantations de deux couches minces ferromagnétiques," C. R. Hebd. Seances Acad. Sci. **255**, 1676–1681 (1962).

32. M. J. Kamali Ashtiani, M. Mokhtarzadeh, M. Hamdi, and S. M. Mohseni, "Morphological magnetostatic coupling in spin valves due to anisotropic self-affine interface roughness," J. Appl. Phys. **127**, 095301 (2020). https://doi.org/10.1063/1.5143407

33. C. Tiusan, M. Hehn, and K. Ounadjela, "Magnetic-roughness-induced magnetostatic interactions in magnetic tunnel junctions," Eur. Phys. J. B **26**, 431–434 (2002). https://doi.org/10.1140/epjb/e20020110

34. S. Goolaup, N. Singh, and A. O. Adeyeye, "Coercivity variation in $Ni_{80}Fe_{20}$ ferromagnetic nanowires," IEEE Trans. Nanotechnol. **4**, 523–526 (2005). https://doi.org/10.1109/TNANO.2005.851405

35. V. A. Orlov, G. S. Patrin, M. V. Dolgopolova, and I. N. Orlova, "Magnetic vortex near the extended linear magnetic inhomogeneity," J. Magn. Magn. Mater. **533**, 167999 (2021). https://doi.org/10.1016/j.jmmm.2021.167999

Translated by O. Kadkin